PLAXIS

essential for geotechnical professionals

PLAXIS

Circular Tunnel Driven in an Elasto-Plastic Isotropic Rock Mass Subjected to Uniform In-Situ Stresses

2016

by

T.D.Y.F. Simanjuntak
Plaxis bv, The Netherlands

1. Introduction

For cases where there is no preferred orientation of joints in a rock mass, the rock mass can be considered to behave as an isotropic medium. This report aims at investigating the mechanical response of an elasto-plastic rock mass as a result of circular excavation subjected to uniform in-situ stresses based on the Hoek-Brown failure criterion.

In cases of deep tunnels, the gravitational force can be assumed negligible due to the fact that the variation of vertical loading across the height of excavation is small compared to the magnitude of the stresses at the excavation location (Detournay and Fairhurst, 1987). Herein, the tunnel being considered is long and has a circular geometry. It is assumed that plane strain conditions are valid along the tunnel axis.

Two cases are investigated based on whether the rock mass behaves as either an elasto-plastic isotropic non-dilatant or a dilatant material. For the former case, the rock mass undergoes no change in volume during plastic deformations, while for the latter case, it does. In view of model validation, the numerical results are compared with those calculated using the closed-form solution.

2. Objectives

The study objectives are:
1. to investigate the behaviour of an elasto-plastic isotropic rock mass to circular excavation subjected to uniform in-situ stresses
2. to study the influence of dilatancy on the rock deformations in the plastic region when the rate of dilation is constant.

3. The Hoek-Brown Failure Criterion

The non-linear Hoek-Brown failure criterion (Hoek and Brown, 1980) is expressed as:

$$\sigma_1 = \sigma_3 + \sigma_{ci}\left(m_b \frac{\sigma_3}{\sigma_{ci}} + s\right)^a \tag{1}$$

σ_{ci} is the uniaxial compressive strength of the intact rock material, and σ_1 and σ_3 represent the major and minor principal stress respectively. Parameters constants m_b and s depend on the structure and surface conditions of the joints in the rock mass, and are given by:

$$m_b = m_i\, e^{(GSI - 100)/(28 - 14D)} \tag{2}$$

$$s = e^{(GSI - 100)/(9 - 3D)} \tag{3}$$

$$a = \frac{1}{2} + \frac{1}{6}\left(e^{-GSI/15} - e^{-20/3}\right) \tag{4}$$

where *GSI* is the Geological Strength Index (Marinos et al., 2005) that takes into account the geometrical shape of intact rock fragments as well as the condition of joint faces, and *D* is the disturbance factor that can vary between 0 (undisturbed) and 1 (disturbed) depending on the amount of stress relief, weathering and blast damage as a result of nearby excavations. For the significance of the parameters and their values, one can refer to Hoek et al., 2002.

If the intact rock modulus, E_i, is known, the rock mass modulus, E_{rm}, can be determined from (Hoek and Diederichs, 2006):

$$E_{rm} = E_i \left(0.02 + \frac{1 - (D/2)}{1 + e^{(60 + 15D - GSI)/11}} \right) \tag{5}$$

Otherwise, the rock mass modulus, E_{rm}, is calculated using (Hoek and Marinos, 2007):

$$E_{rm}\ [MPa] = 10^5 \left(\frac{1 - (D/2)}{1 + e^{(75 + 25D - GSI)/11}} \right) \tag{6}$$

The Hoek-Brown failure surfaces in three-dimensional principal stress space can be piecewise written as (Benz et al., 2008):

$$\begin{aligned} f_{HB,13} &= \sigma_1 - \sigma_3 - \sigma_{ci} \left(m_b \frac{\sigma_3}{\sigma_{ci}} + s \right)^a = 0 \\ f_{HB,12} &= \sigma_1 - \sigma_2 - \sigma_{ci} \left(m_b \frac{\sigma_2}{\sigma_{ci}} + s \right)^a = 0 \end{aligned} \tag{7}$$

The plastic potential function can be defined as (Carranza-Torres and Fairhurst, 1999; Benz et al., 2008):

$$\begin{aligned} g_{HB,13} &= S_1 - \left(\frac{1 + \sin\psi_{mob}}{1 - \sin\psi_{mob}} \right) S_3 \\ g_{HB,12} &= S_1 - \left(\frac{1 + \sin\psi_{mob}}{1 - \sin\psi_{mob}} \right) S_2 \end{aligned} \tag{8}$$

where ψ_{mob} is the mobilised angle of dilatancy and S_i are the transformed stresses.

The transformed stresses, S_i, can be written as (Carranza-Torres and Fairhurst, 1999):

$$S_i = \frac{\sigma_i}{m_b\ \sigma_{ci}} + \frac{s}{m_b^2} \qquad for\ i\ =\ 1, 2, 3 \tag{9}$$

With increasing minor principal stress, the initial angle of dilatancy ψ is reduced to zero in a linear manner ($0 \geq \sigma_3 \geq \sigma_\psi$) (Benz et al., 2008):

$$\psi_{mob} = \frac{\sigma_\psi - (\sigma_3 - \sigma_t)}{\sigma_\psi}\ \psi \geq 0 \tag{10}$$

where σ_ψ and σ_t are the threshold stress and the maximum allowable tensile stress respectively. The tensile stress is determined using:

$$\sigma_t = \frac{\sigma_{ci}\ s}{m_b} \tag{11}$$

In order to allow for plastic expansion in the tensile zone ($\sigma_t \geq \sigma_3 \geq 0$), an increased artificial value of the mobilised dilatancy is used and can be expressed as:

$$\psi_{mob} = \psi + \frac{\sigma_3}{\sigma_t}(90° - \psi) \tag{12}$$

The evolution of the mobilised dilatancy angle as a function of σ_3 is shown in Fig. 1.

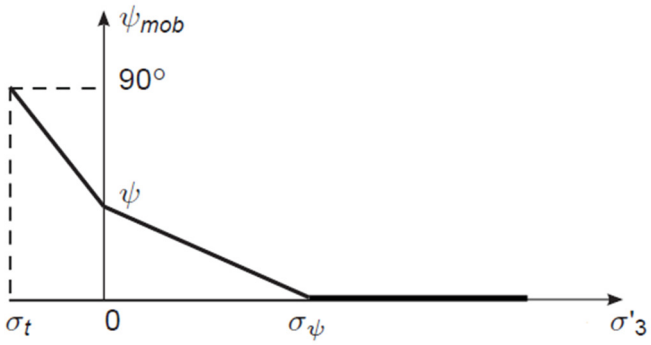

Fig. 1. Evolution of Mobilised Dilatancy Angle

4. Plastic Zone

The total deformations in the rock mass are made up of two components, namely the elastic and plastic component. The radius of elastic-plastic interface, R_{pl}, around a circular excavation can be determined by using (Carranza-Torres and Fairhurst, 1999):

$$R_{pl} = R\, e^{\left[2\left(\sqrt{P_e^{cr}} - \sqrt{P_e}\right)\right]} \tag{13}$$

where P_e and P_e^{cr} are the scaled support pressure and the scaled critical pressure, respectively. They can be calculated using the following equations:

$$P_e = \frac{p_e}{m_b\ \sigma_{ci}} + \frac{s}{m_b^2} \tag{14}$$

$$P_e^{cr} = \frac{1}{16}\left[1 - \sqrt{1 + 16\left(\frac{\sigma_o}{m_b\ \sigma_{ci}} + \frac{s}{m_b^2}\right)}\right]^2 \tag{15}$$

If the critical pressure is higher than the scaled support pressure, plasticity occurs around the excavation. The radial stress at the elastic-plastic interface, $\sigma_{r,Rpl}$, can be obtained as:

$$\sigma_{r,\,R_{pl}} = \left(P_e^{cr} - \frac{s}{m_b^2}\right) m_b\ \sigma_{ci} \tag{16}$$

5. Stresses and Deformation in the Elastic Region

In the elastic region, the radial and hoop stress as well as the radial deformation around the tunnel can be calculated using the Lame's solution, which can be written as (Sharan 2005; Carranza-Torres and Fairhurst, 1999):

$$\sigma_r^{el} = \sigma_o - (\sigma_o - \sigma_{r,R_{pl}}) \left(\frac{R}{r}\right)^2 \tag{17}$$

$$\sigma_\theta^{el} = \sigma_o + (\sigma_o - \sigma_{r,R_{pl}}) \left(\frac{R}{r}\right)^2 \tag{18}$$

$$u_r^{el} = \frac{R^2}{r} \frac{(1+\nu)}{E_{rm}} (\sigma_o - \sigma_{r,R_{pl}}) \tag{19}$$

where σ_o and ν are the mean in-situ stress in the rock mass and the Poisson's ratio of an intact rock respectively.

6. Stresses and Deformation in the Plastic Region

Based on the transformation rule for stresses and the assumption of ideally plastic behaviour of the rock mass, the radial and hoop stresses in the plastic region can be determined using (Carranza-Torres, 2004):

$$\sigma_r^{pl} = \left(\left[\sqrt{P_e^{cr}} + \frac{1}{2} \ln\left(\frac{r}{R_{pl}}\right) \right]^2 - \frac{s}{m_b^2} \right) m_b \, \sigma_{ci} \tag{20}$$

$$\sigma_\theta^{pl} = \left(\left[\sqrt{P_e^{cr}} + \frac{1}{2} \ln\left(\frac{r}{R_{pl}}\right) \right]^2 + \sqrt{P_e^{cr}} + \frac{1}{2} \ln\left(\frac{r}{R_{pl}}\right) - \frac{s}{m_b^2} \right) m_b \, \sigma_{ci} \tag{21}$$

Considering that there is no change in rock mass volume during plastic deformations, the radial deformation in the plastic region can be calculated using (Carranza-Torres and Fairhurst 1999; Carranza-Torres 2004):

$$\begin{aligned} \frac{u_r^{pl}}{R} \frac{E_{rm}}{(1+\nu)\,(\sigma_o - p_e^{cr})} = & \left[\frac{1-2\nu}{2} \frac{\sqrt{P_e^{cr}}}{\left(\frac{\sigma_o}{m_b\,\sigma_{ci}} + \frac{s}{m_b^2}\right) - P_e^{cr}} + 1 \right] \left(\frac{R_{pl}}{R}\right)^2 + \\ & + \frac{1-2\nu}{4\left[\left(\frac{\sigma_o}{m_b\,\sigma_{ci}} + \frac{s}{m_b^2}\right) - P_e^{cr}\right]} \left[\ln\left(\frac{R_{pl}}{R}\right)\right]^2 - \\ & - \frac{1-2\nu}{2} \frac{\sqrt{P_e^{cr}}}{\left(\frac{\sigma_o}{m_b\,\sigma_{ci}} + \frac{s}{m_b^2}\right) - P_e^{cr}} \left[2 \ln\left(\frac{R_{pl}}{R}\right) + 1\right] \end{aligned} \tag{22}$$

For cases of dilatant rocks, the radial deformation in the plastic region is given by (Carranza-Torres and Fairhurst 1999; 2000):

$$\frac{u_r^{pl}}{R}\frac{E_{rm}}{(1+\nu)\,(\sigma_o - p_e^{cr})} = \frac{K_\psi - 1}{K_\psi + 1} + \left(\frac{2}{K_\psi + 1}\right)\left(\frac{R_{pl}}{R}\right)^{K_\psi + 1} + \\ + \frac{1-2\nu}{4\left[\left(\frac{\sigma_o}{m_b\,\sigma_{ci}} + \frac{s}{m_b^2}\right) - P_e^{cr}\right]}\left[\ln\left(\frac{R_{pl}}{R}\right)\right]^2 - \\ - \left[\frac{1-2\nu}{K_\psi + 1}\,\frac{\sqrt{P_e^{cr}}}{\left(\frac{\sigma_o}{m_b\,\sigma_{ci}} + \frac{s}{m_b^2}\right) - P_e^{cr}} + \frac{1-2\nu}{K_\psi + 1}\,\frac{\sqrt{P_e^{cr}}}{\left(\frac{\sigma_o}{m_b\,\sigma_{ci}} + \frac{s}{m_b^2}\right) - P_e^{cr}}\right] \times \\ \times \left[(K_\psi + 1)\ln\left(\frac{R_{pl}}{R}\right) - \left(\frac{R_{pl}}{R}\right)^{K_\psi + 1} + 1\right] \tag{23}$$

where a dilation coefficient K_ψ is calculated using (Carranza-Torres and Fairhurst 1999):

$$K_\psi = \frac{1 + \sin\psi}{1 - \sin\psi} \tag{24}$$

7. Numerical Results

In the following, the mechanical response of both an elasto-plastic isotropic non-dilatant and dilatant rock mass to circular excavation is analysed. The in-situ stresses in the rock mass are uniform and are characterised by a compressive stress of 25 MPa. The radius of excavation, R, is 10 m and the excavation is assumed to result in minimal disturbance. The data for the intact rock are adopted from (Carranza-Torres and Fairhurst, 1999).

The parameter constants m_b, s and a are calculated using Eqs. (2), (3) and (4) respectively, whereas the rock mass modulus E_{rm} was calculated using Eq. (5) since the intact rock modulus is known. The rock mass data used in the analysis are summarised in Table 1.

Table 1. Rock Mass Data (Carranza-Torres and Fairhurst, 1999)

GSI	*D*	σ_{ci} (MPa)	E_i (GPa)	ν_r	m_i	m_b	s	a	E_r (GPa)	σ_o (MPa)
50	0	30	20	0.25	10	1.68	0.004	0.5	6.14	25

Case A – Elasto-Plastic Isotropic Non-Dilatant Rock Mass

a) Excavation-Induced Radial Deformations

Fig. 2 presents the numerical results of excavation-induced radial deformations around the tunnel for cases where the rock mass is assumed to behave as an elasto-plastic isotropic non-dilatant material. The predicted radial deformation along the tunnel perimeter was obtained as 0.23 m or is equal to u_r/R of 2.3%, and is uniformly distributed along the tunnel walls. If calculated using Eq. (23), the radial deformation at the tunnel walls was found as 0.22 m. The distribution of radial deformations in the space around the excavation is shown in Fig. 3. It is evident that the numerical results are in good agreement with those obtained using the closed-form solution.

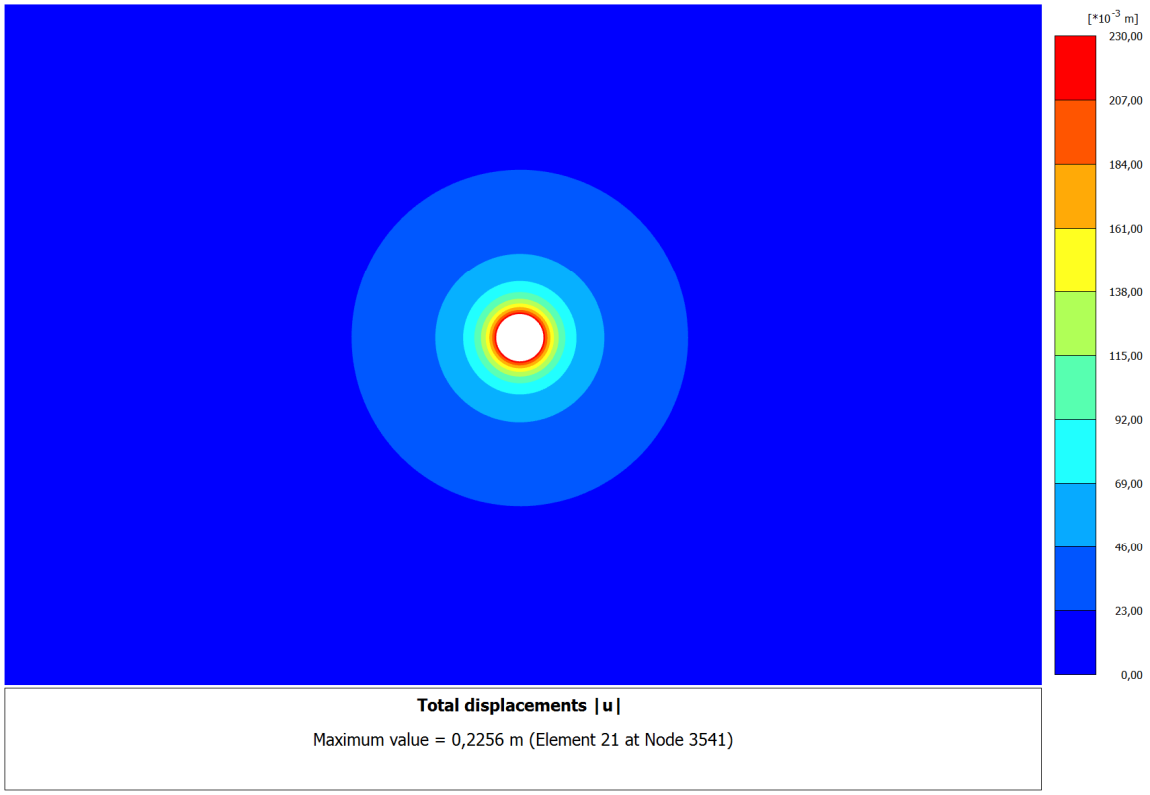

Fig. 2. Predicted Excavation-Induced Radial Deformations (ψ = 0°)

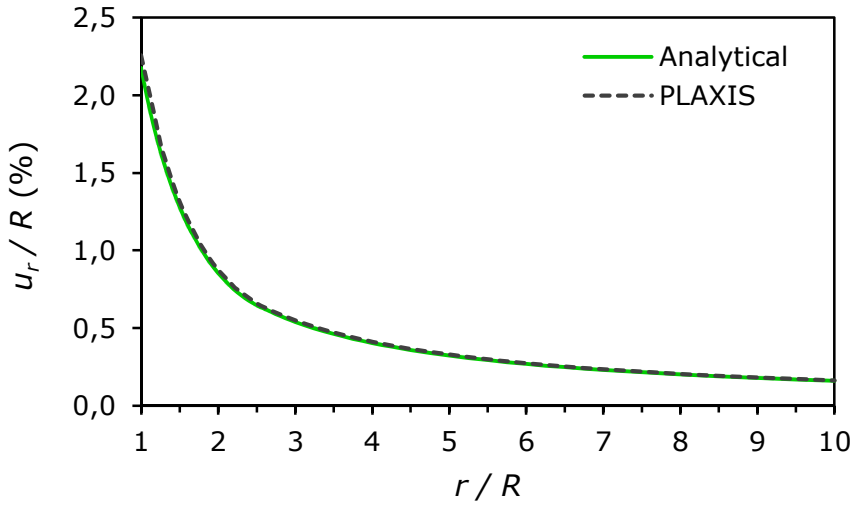

Fig. 3. Distribution of Radial Deformations (ψ = 0°)

b) Excavation-Induced Radial Stresses

The numerical results of excavation-induced radial stresses in the space surrounding the tunnel are depicted in Fig. 4. Since the tunnel is unsupported, the radial stress along the tunnel walls is zero. The radial stress increases towards a value near to the far field stress, i.e. 25 MPa as the tunnel radius increases. For instance, at the distance of 10R, the radial stress was found as 0.97σ_o. Using Eqs. (16), (17) and (20), the radial deformation at the tunnel walls was obtained as 0.97σ_o. The comparison between the analytical and numerical solution is shown in Fig. 5.

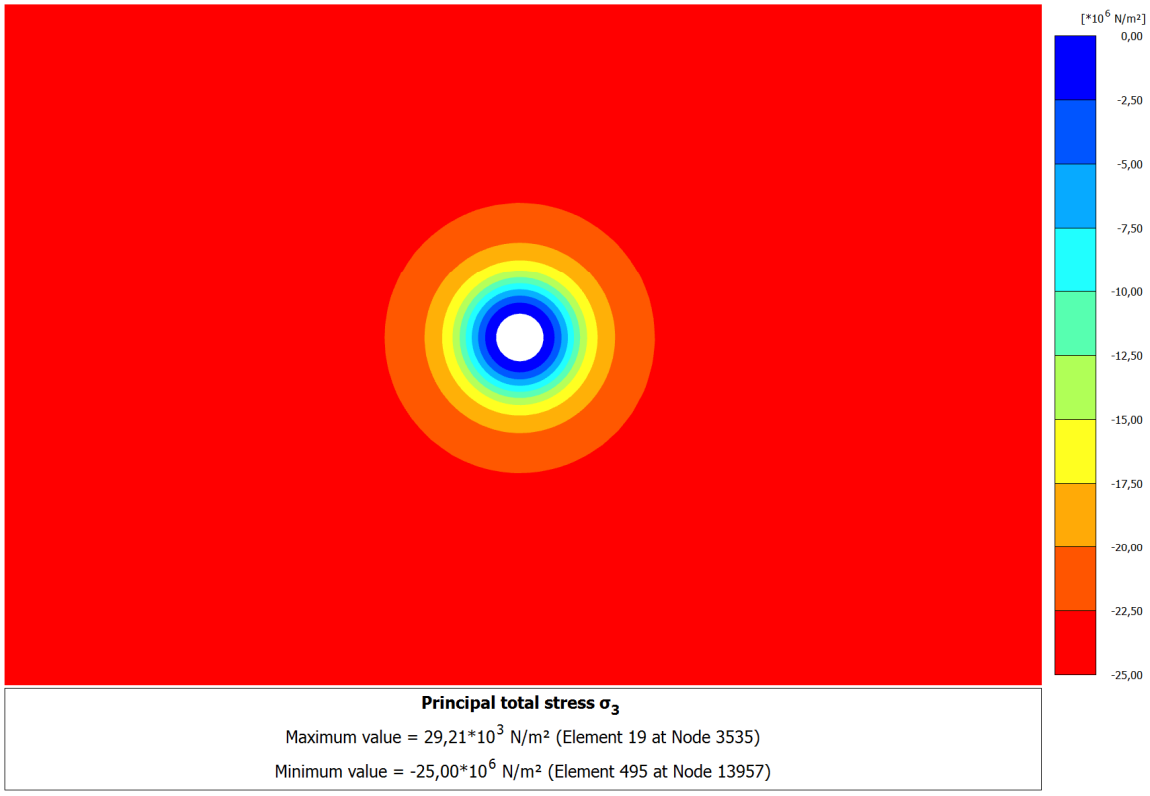

Fig. 4. Predicted Excavation-Induced Radial Stresses (ψ = 0°)

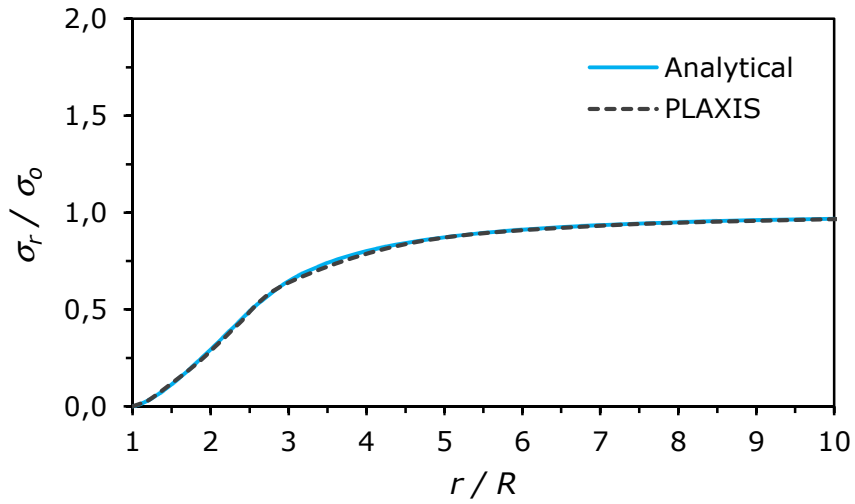

Fig. 5. Distribution of Radial Stresses (ψ = 0°)

c) Excavation-Induced Hoop Stresses

Additionally, the predicted distribution of hoop stresses around the tunnel are shown in Fig. 6. The classical jump indicating the plastic and elastic interface in the rock mass can be seen in Fig. 7. The maximum hoop stress was obtained as $1.50\sigma_o$ and the plastic zone, R_{pl}, was predicted to occur as far as 25.3 m measured from the tunnel centre. When calculated using Eqs. (18) and (21), the hoop stress at the plastic and elastic interface was obtained as $1.50\sigma_o$. The comparison of the distribution of hoop stresses obtained using the numerical and analytical solution is depicted in Fig. 7.

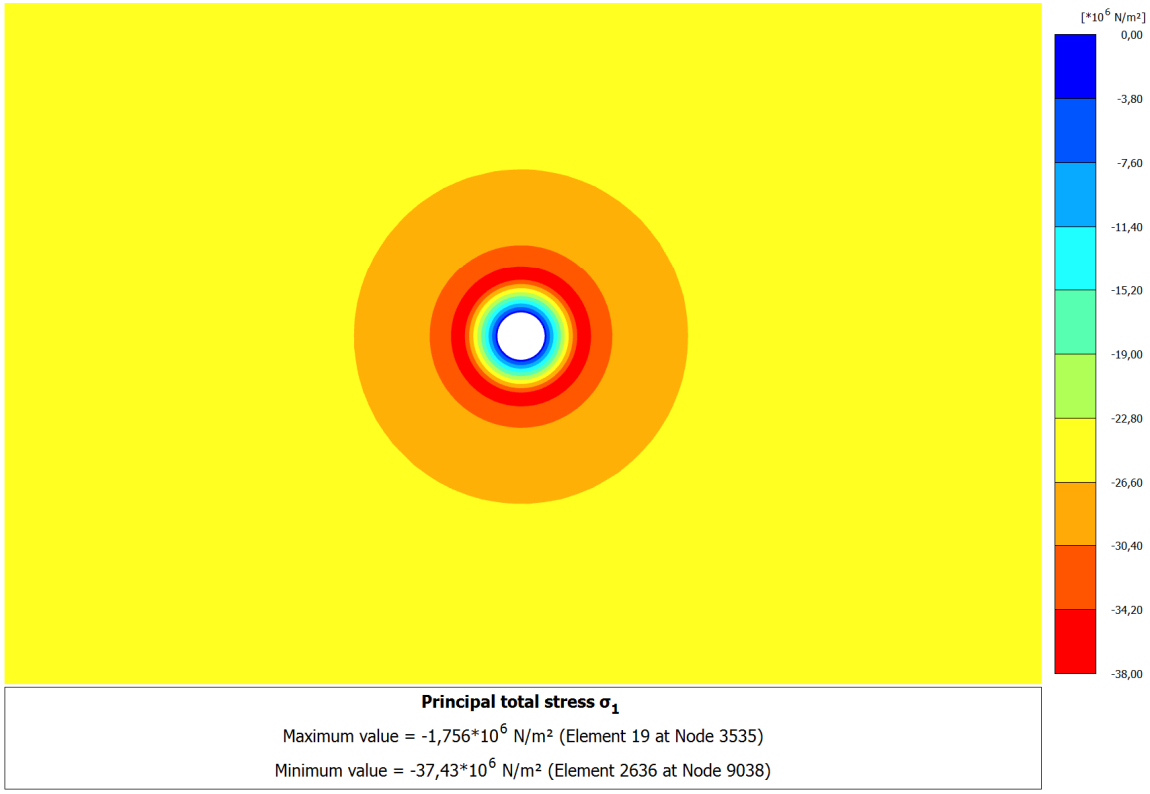

Fig. 6. Predicted Excavation-Induced Hoop Stresses (ψ = 0°)

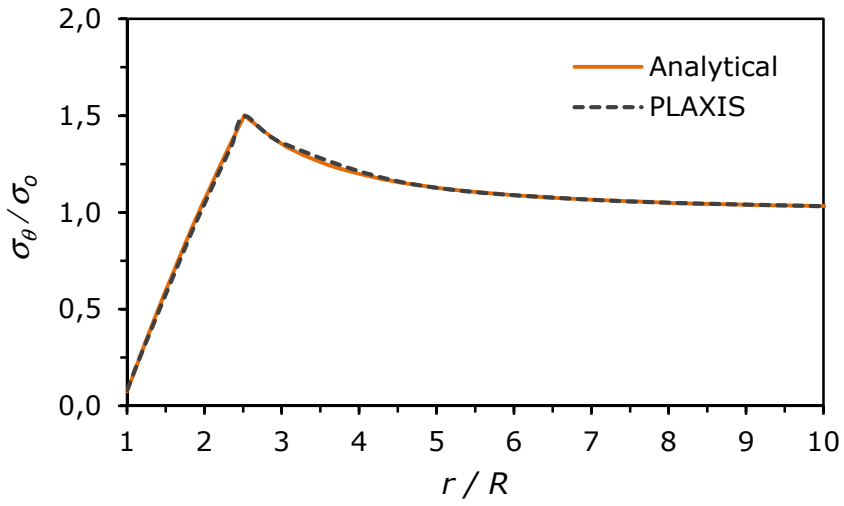

Fig. 7. Distribution of Hoop Stresses (ψ = 0°)

The numerical and analytical results are summarised in Table 2. It is seen that the results obtained using PLAXIS 2D are comparable with those calculated using the closed-form solution with great accuracy. Similar observation can be found in Simanjuntak et al., 2012.

Table 2. Comparison of Results for Cases of Non-Dilatant Rock Mass

Methods	R_{pl} (m)	$u_{r,\ r=0}$ (m)	$\sigma_{r,\ r=10R}$ (MPa)	$\sigma_{\theta,\ r=Rpl}$ (MPa)
Analytical Solutions	25.2	0.22	24.20 (0.97σ_o)	37.55 (1.50σ_o)
PLAXIS	25.3	0.23	24.17 (0.97σ_o)	37.43 (1.50σ_o)

Case B – Elasto-Plastic Dilatant Rock Mass

For cases where the rock mass can be assumed to behave as an elasto-plastic isotropic dilatant material, the numerical results of excavation-induced radial deformations are shown in Fig. 8. In this particular example, the dilation angle was taken as 30°.

In order to have a constant rate of dilation, σ_ψ which is the minor principal stress at which zero volumetric plastic flow is reached, should be set very high, i.e. 50 GPa. The predicted radial deformation at the tunnel walls was found as 0.96 m or it is equal to u_r/R of 9.6%. When calculated using Eq. (23), the radial deformation at the tunnel walls was obtained as 0.93 m.

The distribution of radial deformations in the space around the tunnel is illustrated in Fig. 9. Again, it can be seen that the numerical results are in good agreement with those obtained using the closed-form solution. The comparison of results between the case of non-dilatant material and that of dilatant material is shown in Fig. 10. It is obvious that dilatancy significantly affects the radial deformations in the plastic region.

Table 3. Comparison of Results for Cases of Dilatant Rock Mass

Methods	R_{pl} (m)	$u_{r,\ r\ =\ 0}$ (m)	$\sigma_{r,\ r\ =\ 10R}$ (MPa)	$\sigma_{\theta,\ r\ =\ Rpl}$ (MPa)
Analytical Solutions	25.2	0.93	24.20 ($0.97\sigma_o$)	37.55 ($1.50\sigma_o$)
PLAXIS	25.3	0.96	24.18 ($0.97\sigma_o$)	37.41 ($1.50\sigma_o$)

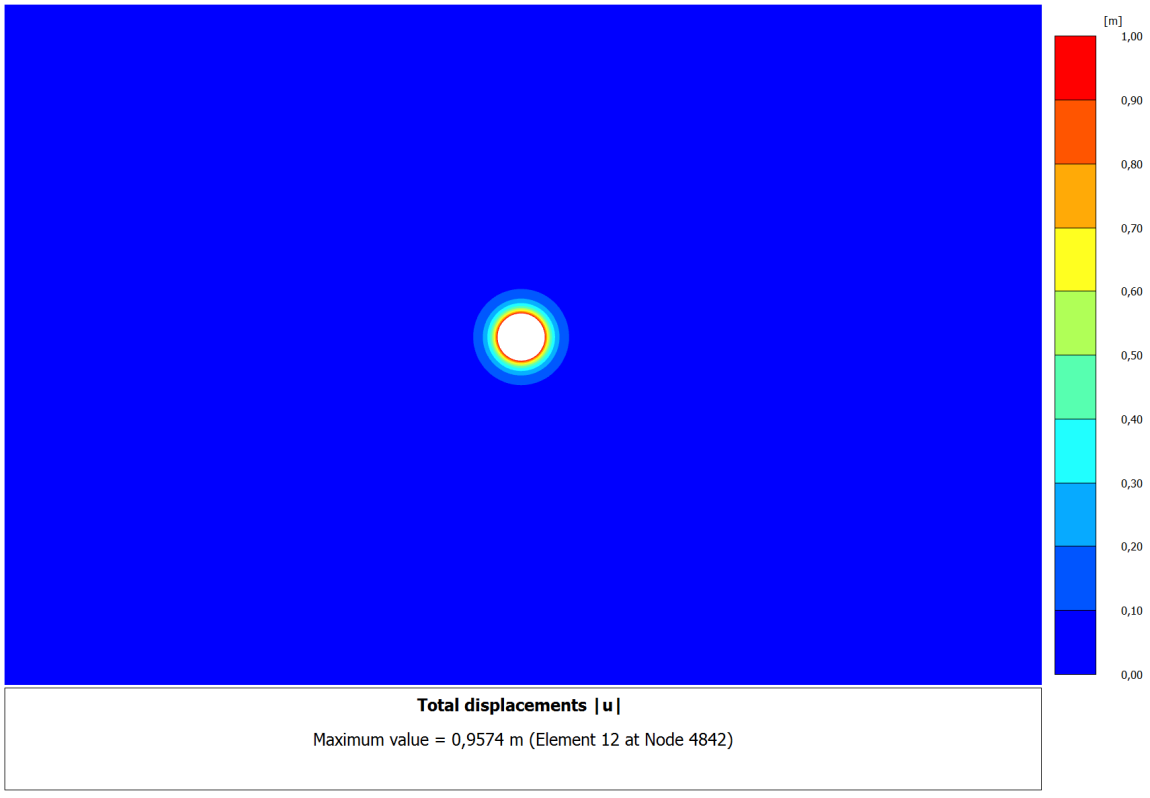

Fig. 8. Predicted Excavation-Induced Radial Deformations (ψ = 30°)

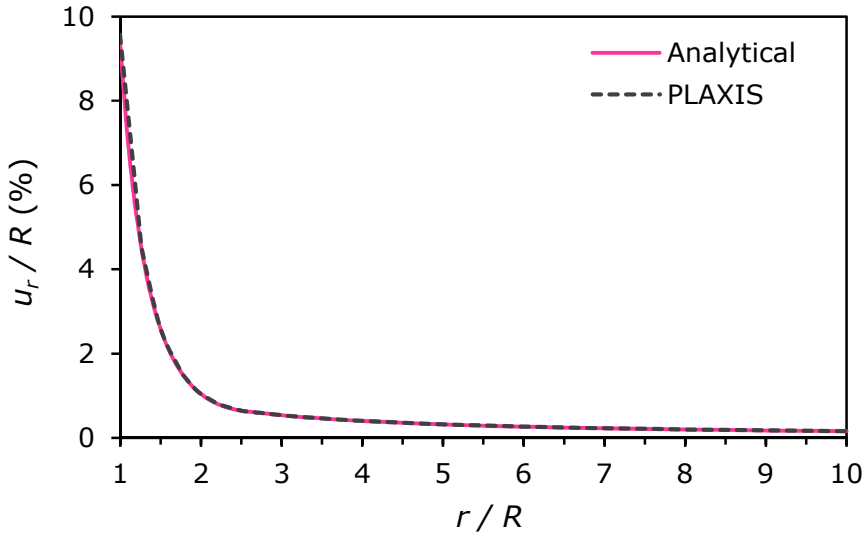

Fig. 9. Distribution of Radial Deformations (ψ = 30°)

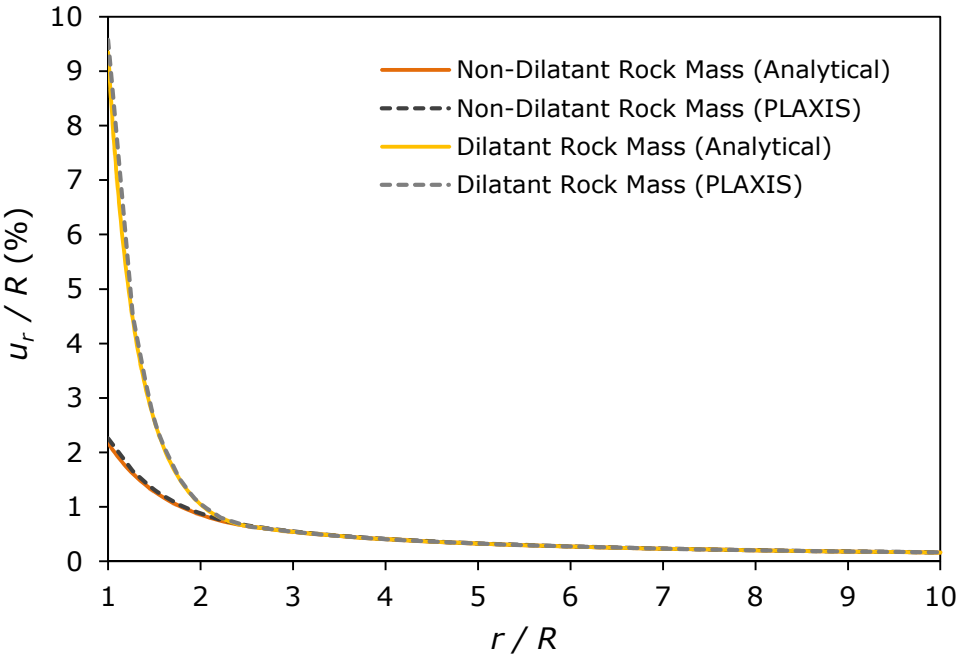

Fig. 10. Comparison of Radial Deformations for Cases of Non-Dilatant and Dilatant Rock Mass

8. Concluding Remarks

This report presents the mechanical response of an elasto-plastic isotropic rock mass to circular excavation using the numerical and analytical solutions. Two cases are distinguished based on whether the rock mass is assumed to behave as a non-dilatant or dilatant material. The bearing capacity of the rock mass was assessed using the Hoek-Brown failure criterion. The tunnel being considered is embedded deep in a dry rock mass where the gravitational force can be assumed negligible.

In view of model validation, the numerical results obtained using PLAXIS 2D are compared against the analytical results calculated using the closed-form solution. This study reports that the numerical results are comparable to the results from the literature with great accuracy, meaning that the approach presented herein are methodologically correct and therefore, can be applied to further investigate the mechanical behaviour of an elasto-plastic isotropic rock mass as a result of circular excavation subjected to non-uniform in-situ stresses.

9. References

Benz, T., Schwab, R., Vermeer, P.A., Kauther, R.A.E. (2008). A Hoek–Brown Criterion with Intrinsic Material Strength Factorization. *International Journal of Rock Mechanics and Mining Sciences*, 45(2), pp. 210–222.

Carranza-Torres, C. (2004). Elasto-Plastic Solution of Tunnel Problems Using the Generalized Form of the Hoek-Brown Failure Criterion. *International Journal of Rock Mechanics and Mining Sciences*, 41, pp. 629–639.

Carranza-Torres, C., Fairhurst, C. (2000). Application of the Convergence-Confinement Method of Tunnel Design to Rock Masses that Satisfy the Hoek-Brown Failure Criterion. *Tunnelling and Underground Space Technology*, 15(2), pp. 187–213.

Carranza-Torres, C., Fairhurst, C. (1999). The Elasto-Plastic Response of Underground Excavations in Rock Masses that Satisfy the Hoek–Brown Failure Criterion. *International Journal of Rock Mechanics and Mining Sciences*, 36(6), pp. 777–809.

Detournay, E., Fairhurst, C. (1987). Two-Dimensional Elasto-Plastic Analysis of a Long, Cylindrical Cavity Under Non-Hydrostatic Loading. In *International Journal of Rock Mechanics and Mining Sciences & Geomechanics Abstracts*. Elsevier, pp. 197–211.

Hoek, E., Brown, E.T. (1980). Empirical Strength Criterion for Rock Masses. *Journal of Geotechnical and Geoenvironmental Engineering*, 106 (ASCE 15715).

Hoek, E., Carranza-Torres, C., Corkum, B. (2002). Hoek-Brown Failure Criterion - 2002 Edition. *Proceedings of NARMS-Tac*, 1, pp. 267–273.

Hoek, E., Diederichs, M.S. (2006). Empirical Estimation of Rock Mass Modulus. *International Journal of Rock Mechanics and Mining Sciences*, 43(2), pp. 203–215.

Hoek, E., Marinos, P. (2007). A Brief History of the Development of the Hoek-Brown Failure Criterion. *Soils and Rocks*, 2, pp. 1–8.

Marinos, V., Marinos, P., Hoek, E. (2005). The Geological Strength Index: Applications and Limitations. *Bulletin of Engineering Geology and the Environment*, 64(1), pp. 55–65.

Sharan, S.K. (2005). Exact and Approximate Solutions for Displacements around Circular Openings in Elastic–Brittle–Plastic Hoek–Brown Rock. *International Journal of Rock Mechanics and Mining Sciences*, 42(4), pp. 542–549.

Simanjuntak, T.D.Y.F., Marence, M., Schleiss, A.J., Mynett, A.E. (2012). Design of Pressure Tunnels Using a Finite Element Model. *The International Journal on Hydropower & Dams*, 19(5), pp. 98–105.